

# Design and Simulation Analysis of Different Shape of Micro Strip Patch Antenna for RFID Application Using Aperture Coupled Technique

BHARANITHARAN.J<sup>1</sup>, JOTHILAKSHMI.P<sup>2</sup>  
*ME-Communication Systems<sup>1</sup>, Assisant Professor<sup>2</sup>*  
*SVCE, Chennai-602 117.*  
*Email:bharanitharan92@gmail.com<sup>1</sup>*

**Abstract-** Different patch of microstrip antenna based on aperture coupled feeding technique is analyzed for RFID application. In aperture coupled feeding mechanisms, the small rectangular slot is etched onto the ground plane for couple the energy between feed line and reference patch. The wave from the slot will radiate the patch and achieve the desired dual band. The air gap is used to avoid the coupling problem between aperture slot and patch. The triangular patch achieved maximum bandwidth of 421.54MHz at designed frequency 5.8GHz. Various structure of microstrip patch antenna such as square patch, triangular patch, rectangular patch, 45<sup>0</sup> rotated square patch and circular patches are designed and analyzed simulated result for RFID(5.8GHz).

## 1. INTRODUCTION

Wireless communication technology is an advancing field and it demand in commercial and military applications. Micro strip patch antennas are used in many wireless communication technologies such as WLAN, WiMAX and RFID applications. The micro strip antenna has advantage of light weight, low volume, low fabrication cost, easy to mount, conformal and low profile. Even though micro strip antenna has compact and light weight in size, it has back radiation problem. To overcome this back lobe radiation problem, aperture Couple feeding technique is used. Using this technique, it reduces back lobe radiation and also increases bandwidth of proposed antenna. It is based on indirectly couple the patch antenna with micro strip line. This contains two substrates connected together with a ground in between, radiating patch is etched on top whereas feed line is on bottom substrate and small aperture in the ground plane couples the patch with feed line. Thus aperture coupled micro strip line reduces the back radiation and mainly, it improves bandwidth and its radiation pattern. In this paper, micro strip patch antenna has been designed for ISM band (RFID) applications.

Radio Frequency Identification (RFID) is a technology that has an advantage of longer range data transfer with high data rates at high frequencies. Many Frequency bands assigned to RFID applications are 125 KHz, 13.56 MHz, 869 MHz, 902-928 MHz, 2.45 (2.400-2.483) GHz, 5.800 (5.72-5.875) GHz. This RFID technology along with aperture coupled micro strip line will be useful to design a compact size antenna that provides high

bandwidth and improved radiation pattern than the other feed lines techniques.

## 2. DESIGN SPECIFICATIONS

The calculations of micro strip patch antenna length are based on transmission line model. Fig.1 shows general micro strip patch antenna with square shape patch. Fig.2 shows left side view of general aperture coupled micro strip patch. Fig.3 shows right side view of aperture coupled micro strip patch.

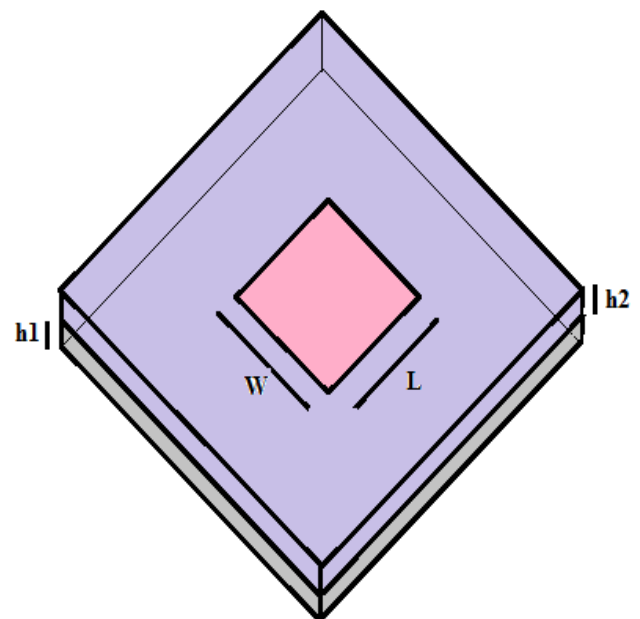


Fig.1 General Micro Strip Patch Antenna

Actual length of the patch and effective length of micro strip antenna can be calculated by equations (1) and (2).

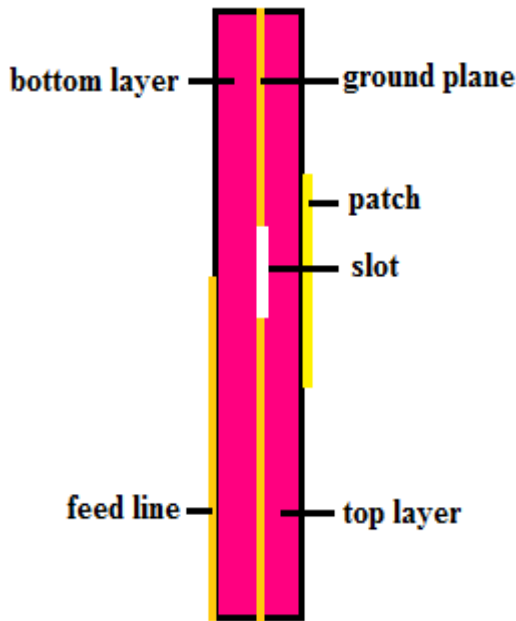


Fig.2 Left Side View of Aperture Coupled Micro Strip Patch Antenna

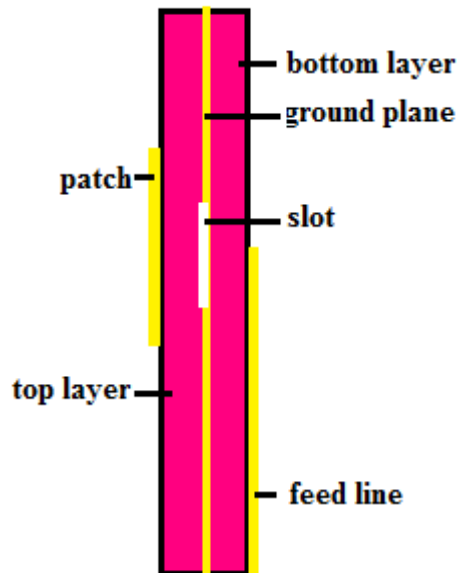


Fig.3 Right Side View of Aperture Coupled Micro Strip Patch Antenna

$$L_{eff} = \frac{c}{2 f_r \sqrt{\epsilon_{eff}}} \quad \dots E.eq.(1)$$

$$L = L_{eff} - 2 \Delta L \quad \dots E.eq.(2)$$

Where  $L_{eff}$  is the effective length,  $\Delta L$  is the extension of length and  $c$  is the velocity of light ( $3 \times 10^8$ ). The width of the micro strip antenna calculated by using equation (3).

$$W = \frac{c}{2 f_r \sqrt{\frac{(\epsilon_r + 1)}{2}}} \quad \dots E.eq.(3)$$

Where  $c$  is the velocity of light ( $3 \times 10^8$  m/s),  $\epsilon_r$  is the dielectric constant of the substrate  $\epsilon_r = 4.4$  and  $f_r$  is the resonant frequency. Effective Dielectric constant of the Micro strip is determined by equation (4).

$$\epsilon_{reff} = \frac{(\epsilon_r + 1)}{2} + \frac{(\epsilon_r - 1)}{2} \left[ 1 + 12 \frac{h}{W} \right]^{-\frac{1}{2}} \quad \dots E.eq.(4)$$

Where  $\epsilon_r$  is the dielectric constant of the substrate  $\epsilon_r = 4.4$ ,  $h$  is the height of the substrate and  $W$  is the width of the substrate. Extension of the length ( $\Delta L$ ) is determined by equation (5).

$$\Delta L = \frac{0.412 * h (\epsilon_{reff} + 0.3) \left( \frac{W}{h} + 0.264 \right)}{(\epsilon_{reff} - 0.258) \left( \frac{W}{h} + 0.8 \right)} \quad E.eq (5)$$

Where,  $\epsilon_{eff}$  is the effective dielectric constant of  $\epsilon_r$  substrate. The substrate used in modelling the entire antenna structure has height of 1.6mm. Fig.4-8 shows different patches of micro strip antenna such as square patch, rectangular patch, diamond patch, triangular patch and circular patch.

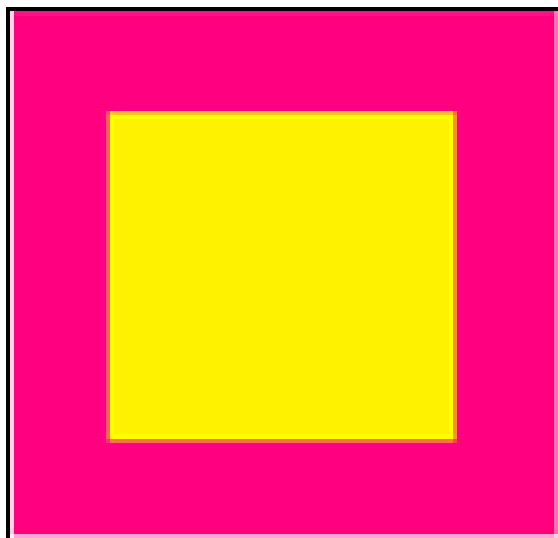


Fig.4 Layout of Square patch antenna

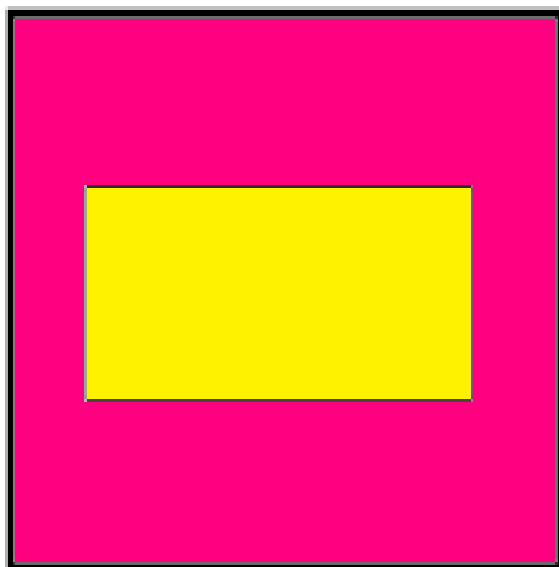


Fig.5 Layout of Triangular patch antenna

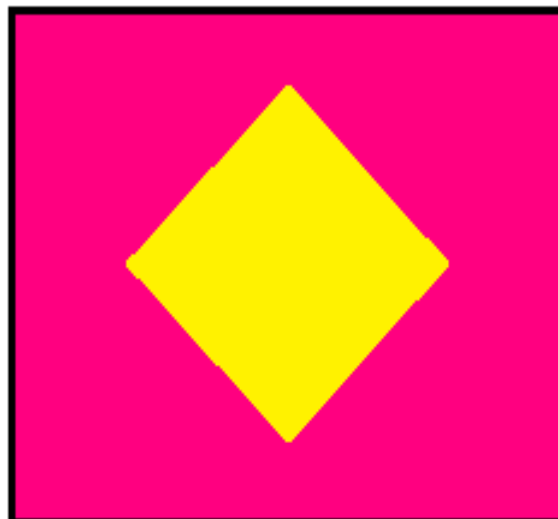


Fig.6 Layout of 45<sup>0</sup> rotated square patch antenna

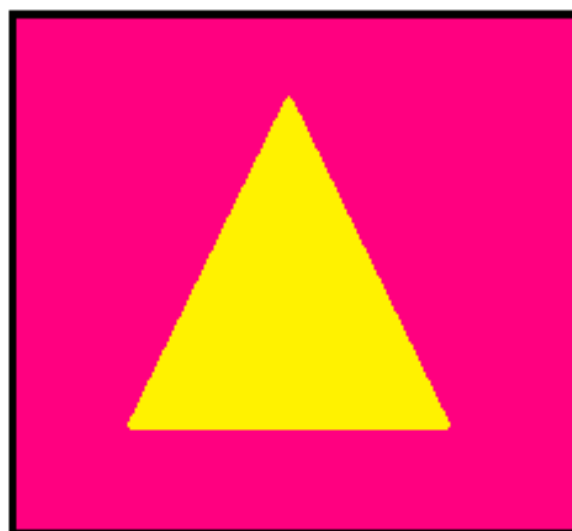


Fig.7 Layout of Diamond patch antenna

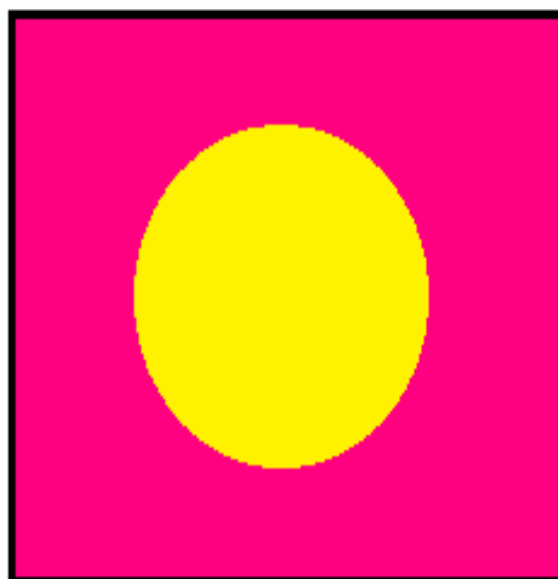


Fig.8 Layout of Circular patch antenna

Fig.9 shows return loss of various patch structure. The maximum return loss of -40.11 at 5.8197GHz achieved by triangular patch. Table.1 shows return loss and bandwidth of various patch structure such as triangular, square, rectangular, diamond, circle patches. The maximum bandwidth 421.54MHz is achieved by triangular patch.

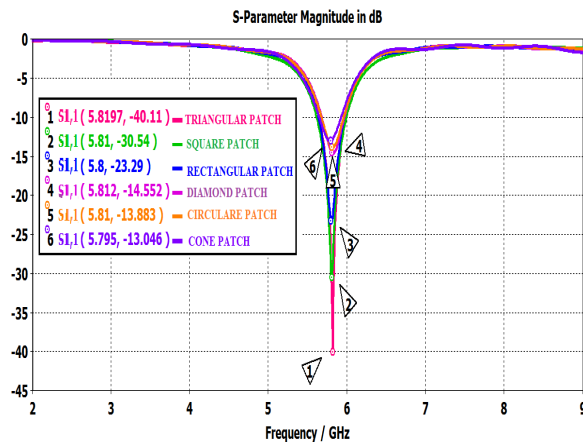


Fig.9 Comparison of return loss

Table.1 comparison of return loss and bandwidth

S.no	Patch	Frequency (GHz)	Return loss	Bandwidth (MHz)
1	Triangular	5.8197	-40.11	421.54
2	Square	5.8	-30.54	403.5
3	Rectangular	5.8068	-23.29	386.48
4	Diamond	5.812	-14.55	346.22
5	Circle	5.81	-13.88	321.54

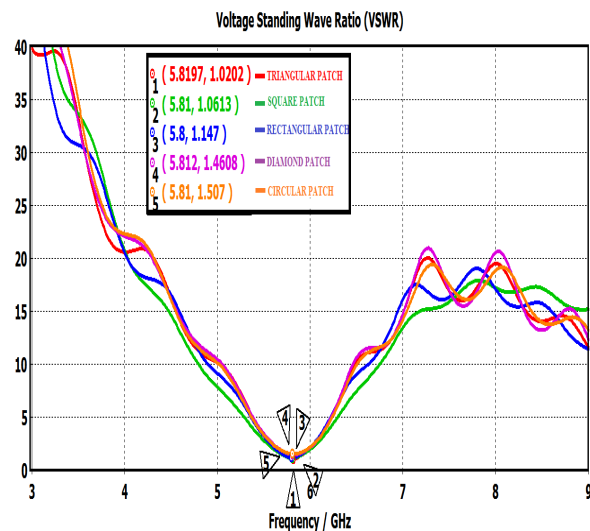


Fig.10 Comparison of VSWR

Table.2.VSWR values for various patch

S.no	Patch	Frequency(GHz)	VSWR
1	Triangular	5.8197	1.0202
2	Square	5.8	1.0613
3	Rectangular	5.8068	1.1470
4	Diamond	5.812	1.4608
5	Circle	5.81	1.5070

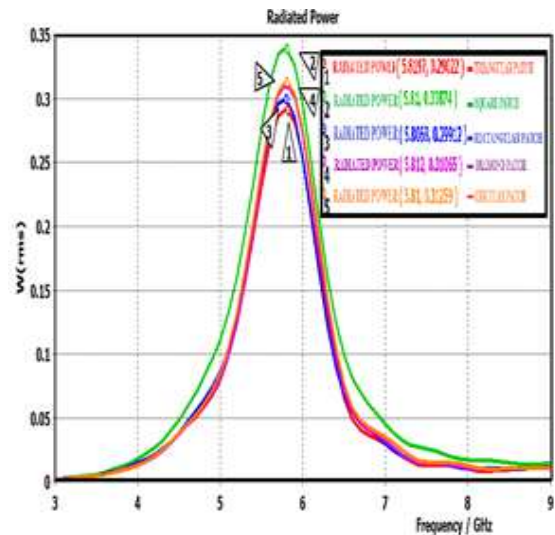


Fig.11. Comparison of radiated power

Table.3.Radiated power values for various patches

S.No	Patch	Radiated Power
1	Triangular	0.29022
2	Square	0.33874
3	Rectangular	0.29912
4	Diamond	0.31065
5	Circle	0.31259

Table.4.Gain and Directivity power values for various patches

S.no	Patch	Gain (dB)	Directivity(dBi)
1	Triangular	3.537	5.861
2	Square	4.171	5.839
3	Rectangular	3.67	5.866
4	Diamond	3.962	5.849
5	Circle	3.941	5.781

Fig.10 shows VSWR of various patch structure. The triangular patch is achieved VSWR of 1.0202. Table.2 shows VSWR of various patch structure such as triangular, square, rectangular, diamond, circle patches. Fig.11 shows Radiated power of various patch structure. The square patch is achieved maximum radiated power of 0.33874. Table.3 shows radiated power of various patch structure such as triangular, square, rectangular, diamond, circle patches.

Table.5.Comparison E field-X,Y,Z

S.No	PATCH	E FIELD X	E FIELD Y	E FIELD Z
1	TRIANGULAR	15983.4	21063.4	114657
2	SQUARE	9950.17	10501	9370.07
3	RECTANGULAR	13806.1	14809.8	13245.1
4	DIAMOND	12404.8	18764.9	15801.1
5	CIRCLE	15983.4	21063.4	11465.7

Table.6.Comparison H field-X,Y,Z.

S.No	PATCH	H FIELD X	H FIELD Y	H FIELD Z
1	TRIANGULAR	60.7257	35.0012	75.2717
2	SQUARE	64.5024	35.4645	84.9545
3	RECTANGULAR	64.785	40.5633	97.5418
4	DIAMOND	58.774	34.9503	83.222
5	CIRCLE	60.7257	35.2012	75.2717

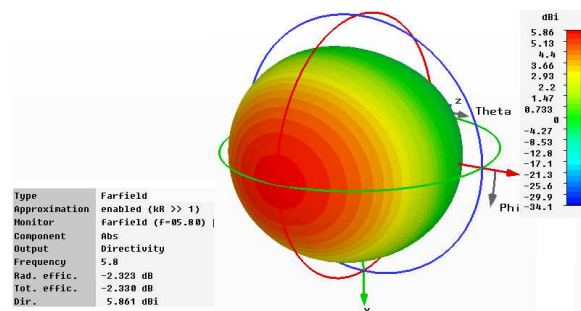


Fig.12.Directivity of triangular patch

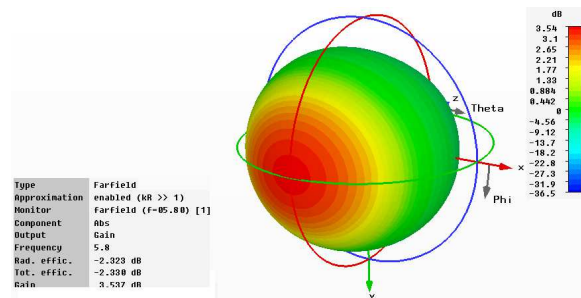


Fig.13.Gain of triangular patch

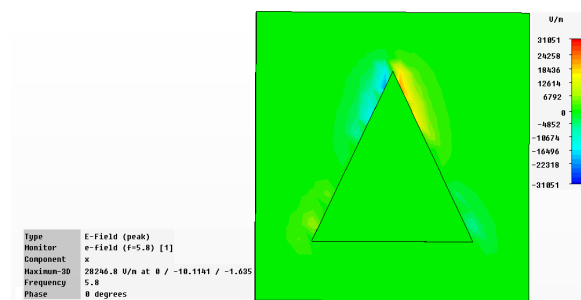


Fig.14.E-field in X direction of triangular patch

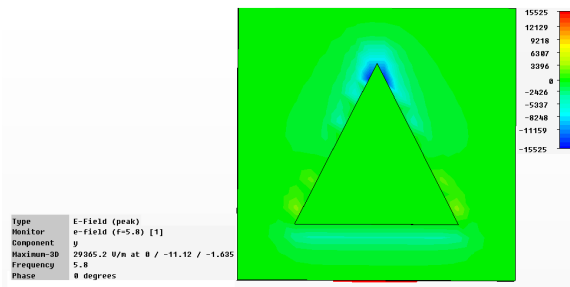


Fig.15.E-field in Y direction of triangular patch

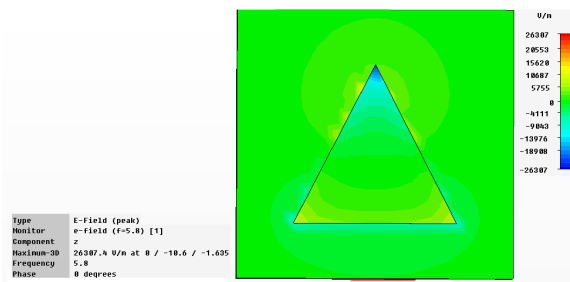


Fig.16.E-field in Z direction of triangular patch

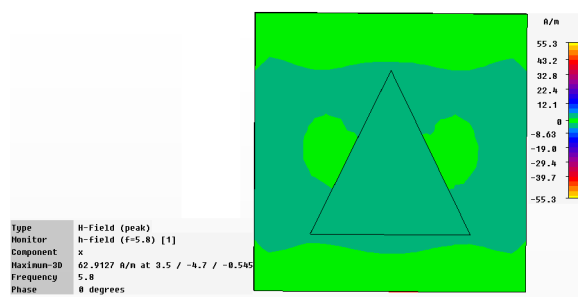


Fig.17.H-field in X direction of triangular patch

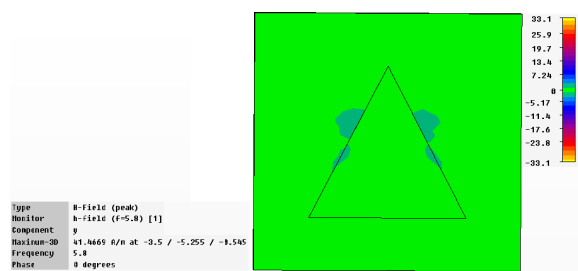


Fig.18.H-field in Y direction of triangular patch

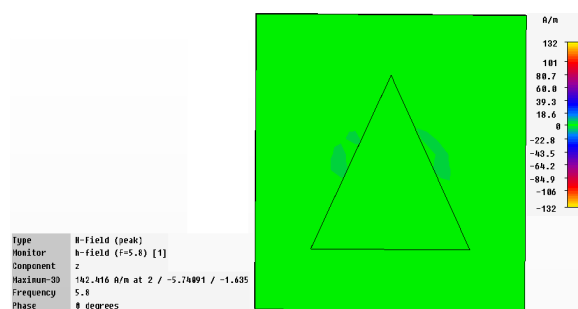


Fig.19.H-field in Z direction of triangular patch

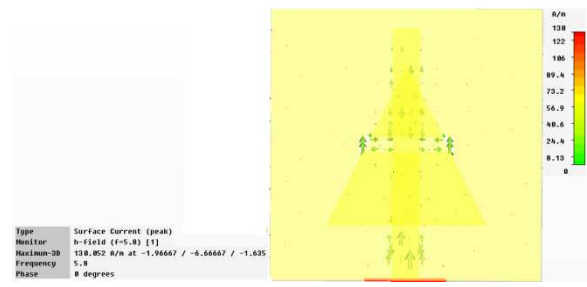


Fig.20.Surface current of triangular patch

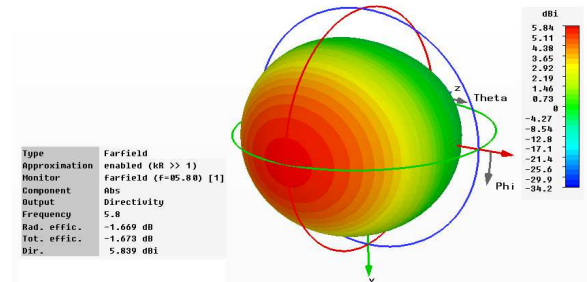


Fig.21.Directivity of square patch

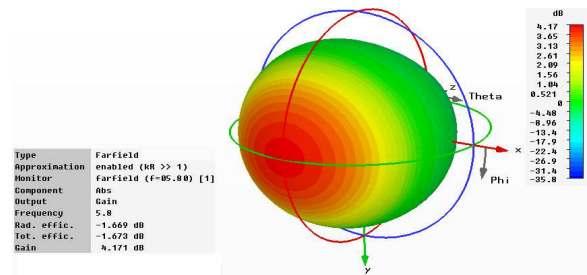


Fig.22.Gain of triangular patch

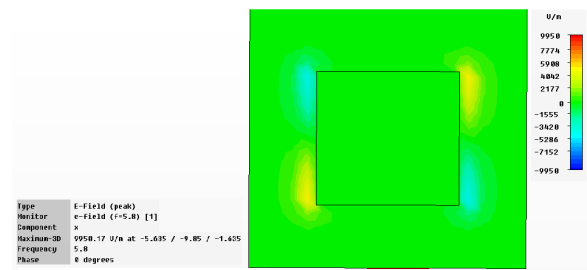


Fig.23.E-field in X direction of square patch

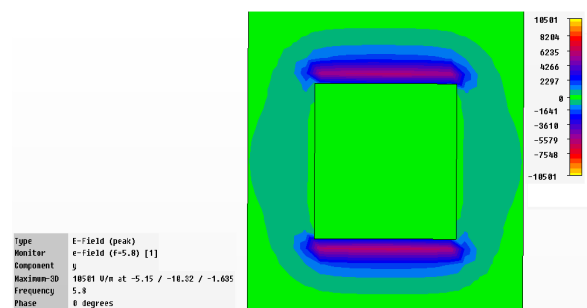


Fig.24.E-field in Y direction of square patch

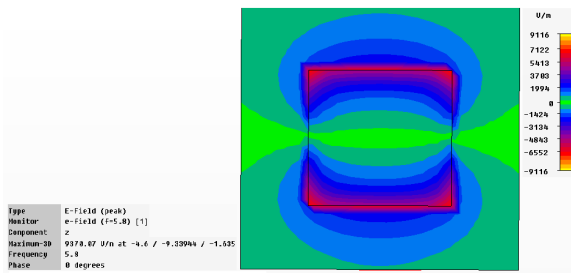


Fig.25.E-field in Z direction of square patch

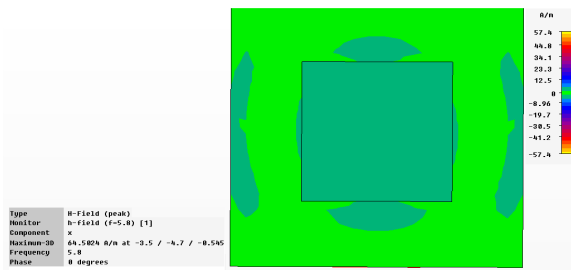


Fig.26.H-field in X direction of square patch

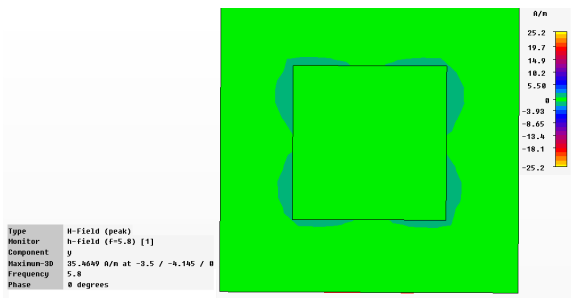


Fig.27.H-field in Y direction of square patch

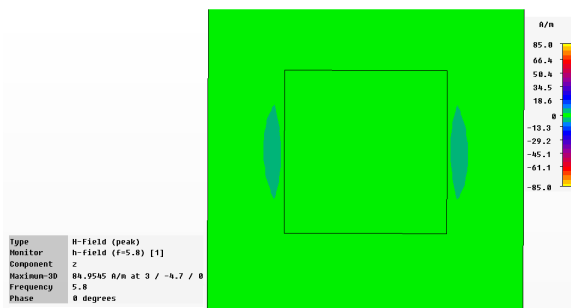


Fig.28.H-field in Z direction of square patch

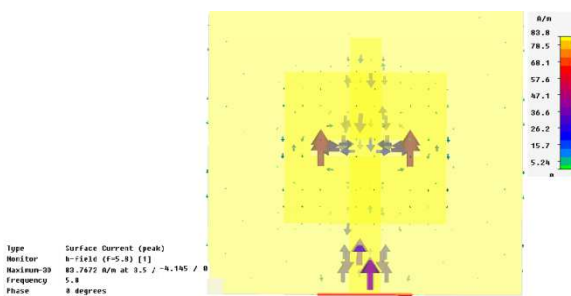


Fig.29.Surface current of square patch

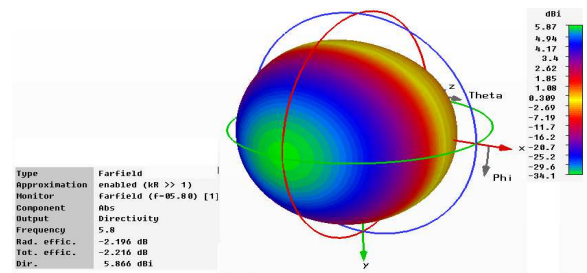


Fig.30.Directivity of rectangular patch

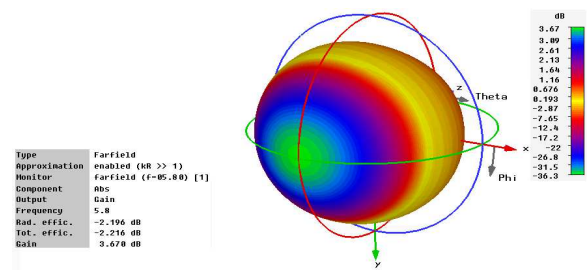


Fig.31.Gain of rectangular patch

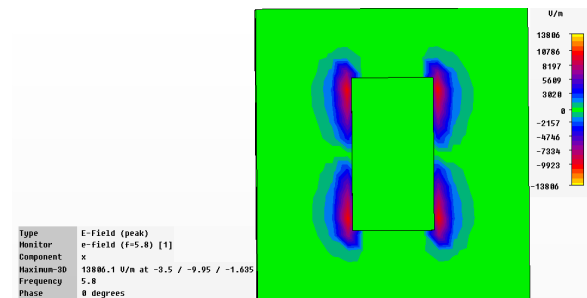


Fig.32.E-field in X direction of rectangular patch

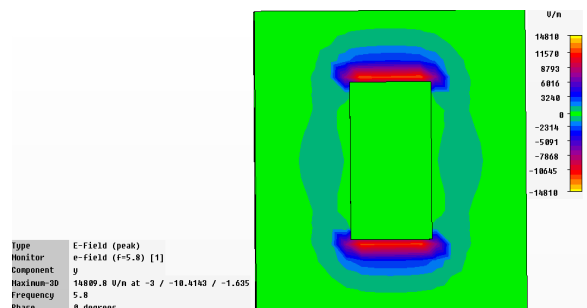


Fig.33.E-field in Y direction of rectangular patch

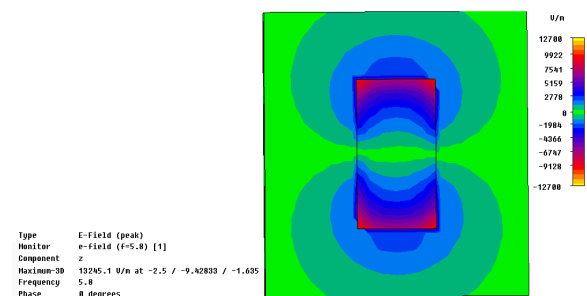


Fig.34.E-field in Z direction of rectangular patch

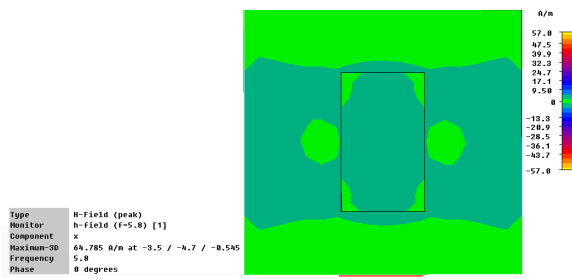


Fig.35.H-field in X direction of rectangular patch

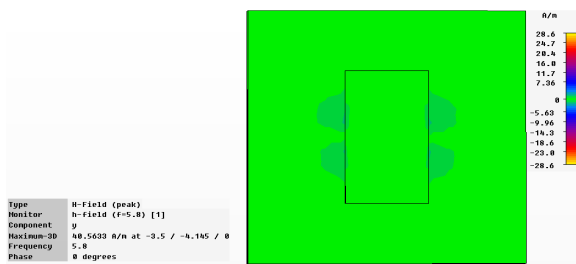


Fig.36.H-field in Y direction of rectangular patch

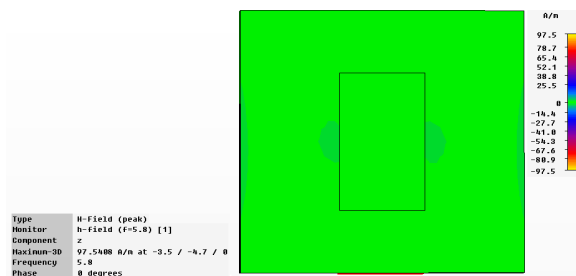


Fig.37.H-field in Z direction of rectangular patch

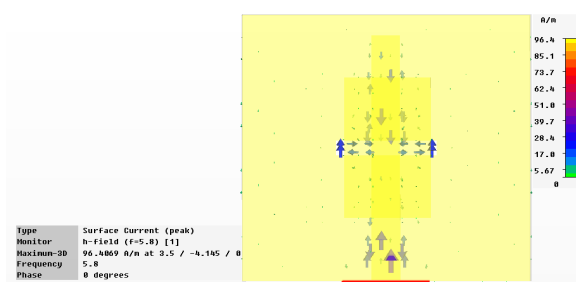


Fig.38.Surface current of rectangular patch

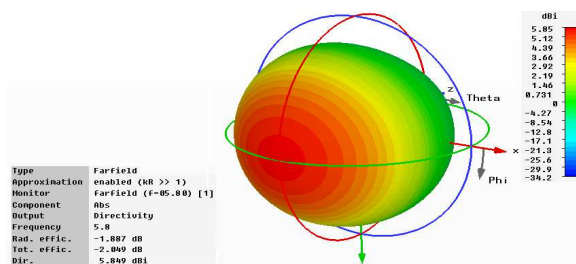


Fig.39.Directivity of 45° rotated square patch

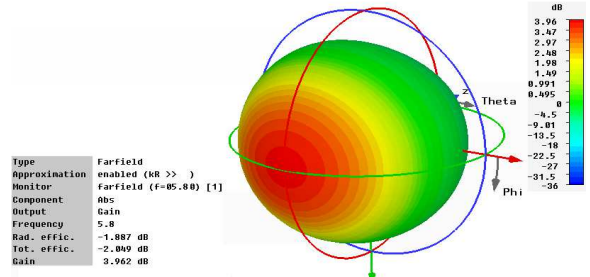


Fig.40.Gain of 45° rotated square patch

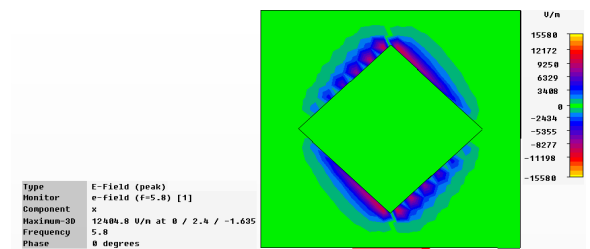


Fig.41.E-field in X direction of 45° rotated square patch

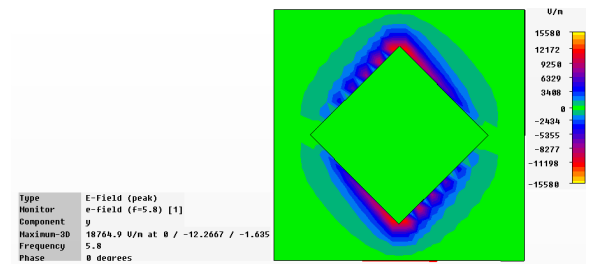


Fig.42.E-field in Y direction of 45° rotated square patch

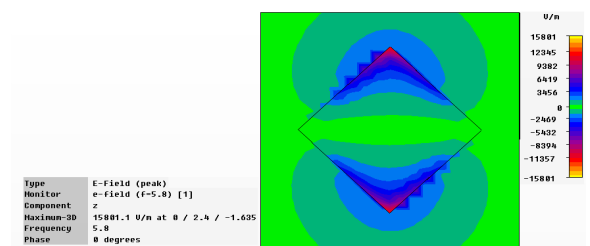


Fig.43.E-field in Z direction of 45° rotated square patch

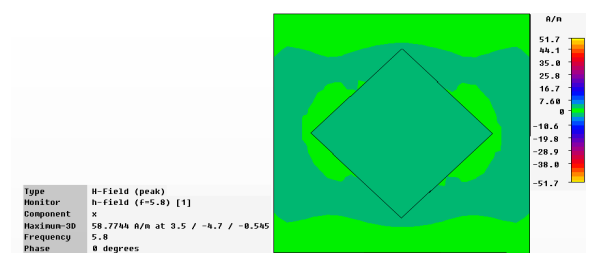


Fig.44.H-field in X direction of 45° rotated square patch



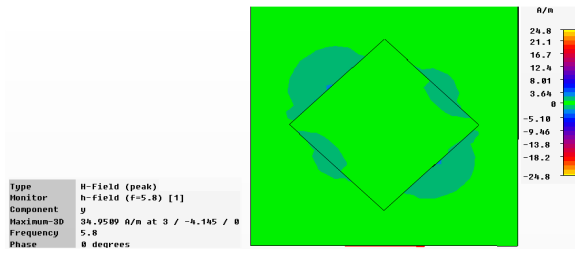


Fig.45.H-field in Y direction of 45° rotated square patch

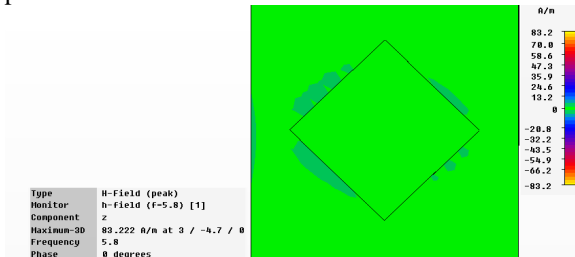


Fig.46.H-field in Z direction of 45° rotated square patch

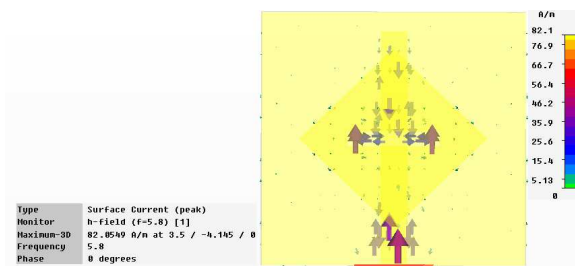


Fig.47.Surface current of 45° rotated square patch

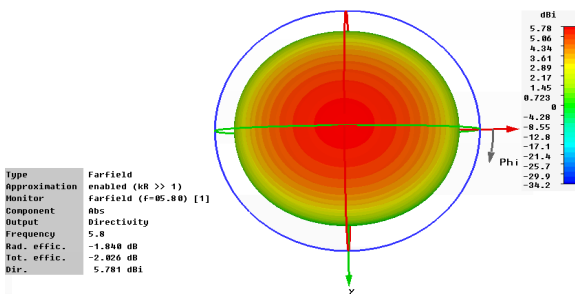


Fig.48.Directivity of circular patch

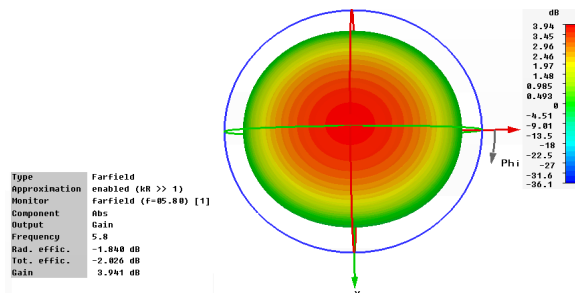


Fig.49.Gain of circular patch

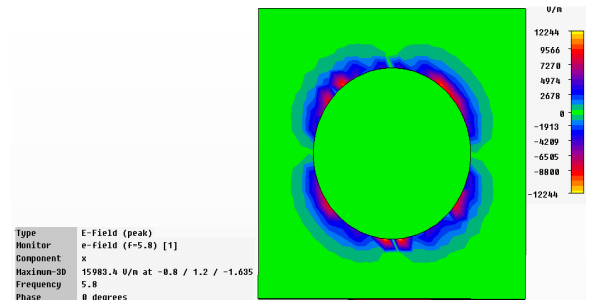


Fig.50.E-field in X direction of circular patch

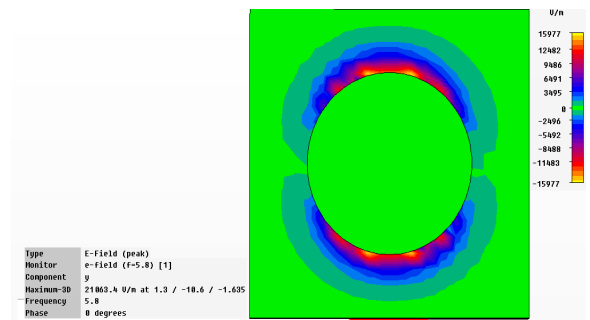


Fig.51.E-field in Y direction of circular patch

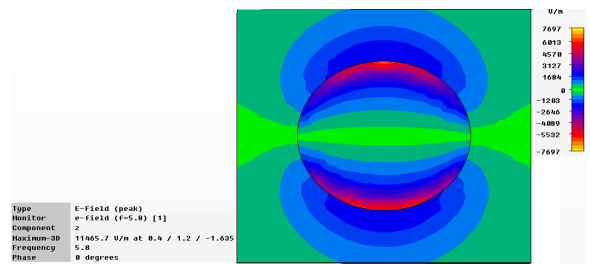


Fig.52.E-field in Z direction of circular patch

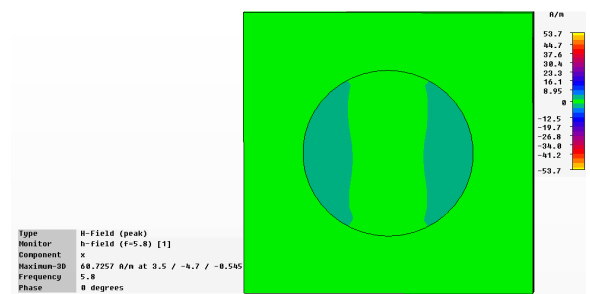


Fig.53.H-field in X direction of circular patch

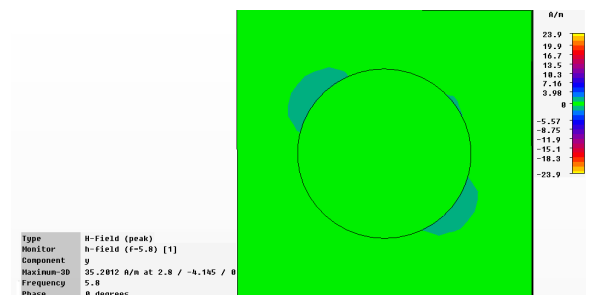


Fig.54.H-field in Y direction of circular patch

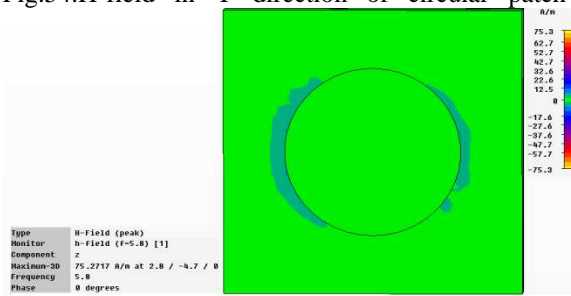


Fig.55.H-field in Z direction of circular patch

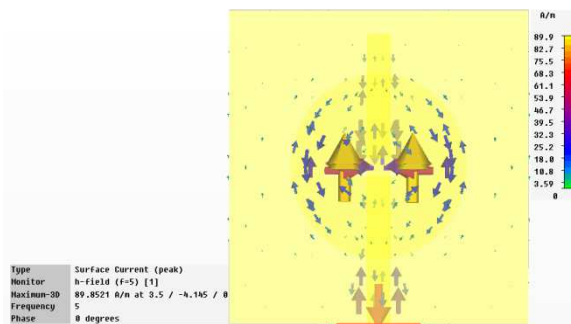


Fig.56.Surface current of circular patch

Fig.10 shows VSWR of various patch structure. The triangular patch is achieved VSWR of 1.0202. Fig.11 shows Radiated power of various patch structure. The square patch is achieved maximum radiated power of 0.33874. The square patch is achieved maximum gain of 4.171dB. Table.2 shows radiated power, VSWR, gain and directivity of various patch structure such as triangular, square, rectangular, 45° rotated square patch, circle patches. Table 3 shows comparison of E field and H field-X, Y and Z direction of various patch structure such as triangular, square, rectangular, 45° rotated square patch and circle patches.

Fig.12 and fig.13 shows 3D view of directivity and gain of triangular patch. Fig.14 to fig.16 shows E field in X, Y and Z direction of triangular patch and fig.17 to 19 shows H field in X, Y and Z direction of triangular patch. Fig.20 shows surface current distribution of triangular patch. Fig.21 and fig.22 shows 3D view of directivity and gain of square patch. Fig.23 to fig.25 shows E field in X, Y and Z direction of square patch and fig.26 to 28 shows H field in X, Y and Z direction of square patch. Fig.29 shows surface current distribution of square patch. Fig.30 and fig.31 shows 3D view of directivity and gain of rectangular patch. Fig.32 to fig.34 shows E field in X, Y and Z direction of rectangular patch and fig.35 to 37 shows H field in X, Y and Z direction of rectangular patch. Fig.38 shows surface current distribution of rectangular patch. Fig.39 and fig.40 shows 3D view of

directivity and gain of 45° rotated square patch. Fig.41 to fig.42 shows E field in X, Y and Z direction of 45° rotated square patch and fig.43 to 45 shows H field in X, Y and Z direction of 45° rotated square patch. Fig.47 shows surface current distribution of circular patch. Fig.48 and fig.49 shows 3D view of directivity and gain of 45° rotated square patch. Fig.50 to fig.52 shows E field in X, Y and Z direction of circular patch and fig.53 to 55 shows H field in X, Y and Z direction of circular patch. Fig.56 shows surface current distribution of 45° circular patch.

### 3. CONCLUSION

Various structures of microstrip patch antenna such as square patch, triangular patch, rectangular patch, 45° rotated square patch and circular patches are designed and simulated for RFID (5.8GHz). From the above the result triangular patch is achieved better result when compared with other structures of microstrip patches such as square, rectangular, 45° rotated square patch and circular patch. The aperture coupled feeding mechanisms is used to achieve the maximum bandwidth of microstrip patch antenna and used in RFID applications.

### REFERENCES

- [1] Amin, Y., q. Chen, H. Tenhunen, and L. R. Zheng, "Performance optimized quadrate bowtie RFID antennas for cost-effective and eco-friendly industrial applications". *Progress In Electromagnetics Research*, Vol, 126, 49-64, 2012.
- [2]. Aslam, A., Bhatti, F.A., (2010), Novel inset feed design technique for Microstrip patch antenna, *International Conference on Applications of Electromagnetism and Student Innovation Competition Awards*, pp 215 – 219
- [3]. Arya, Ashwini K., Patnaik, A. and Kartikeyan, M.V.(2011), "Microstrip Patch Antenna With Skew-F Shaped DGS for Dual Band operation", *Progress In Electromagnetics Research M*, Vol.19, 2011, pp. 147-160.
- [3]. Arya, Patnaik, A. and Kartikeyan, M.V.(2010), "On the Size Reduction of Microstrip Antenna Using DGS", *Proceedings of IEEE Conference*, 2010.
- [4]. Cho, C., H. Choo, and I. Park, "Design of planar RFID tag antenna for metallic objects", *Electronic Letters*, Vol, 4, 175-177, Jan. 2008.
- [5] Franciscatto and T.P.Vuong ; G. Fontagalland.(2011), High Gain Sierpinski Gasket fractal shape antenna designed for RFID , *IEEE Conference* ,2011.
- [6]. Kim, T.H. and D. C. Park, "CPW –fed compact monopole antenna for dual-band WLAN applications", *Electronic Letters*, Vol. 41, No. 6, 291-293, March 17, 2005.

- [7].Li, X, and J. Liao, "Eye-shaped segmented reader antenna for near-field UHF RFID applications", *Progress In Electromagnetics Research*, Vol, 114, 481-493, 2011.
- [8].Lee, H. and Lim, Y. (2001), "Design of circular polarized Microstrip aperture coupled patch antenna for 5.8 GHz ISM band". *Asia-Pacific Microwave Conference*, Vol, 1, 732-733, 2001, pp, 220-223.
- [9].Lee, C. P., Chakrabarty, C.K. and Khan, R.A., (2009), Design of Ultra Wideband slotted microstrip patch antenna, *IEEE 9<sup>th</sup> Malaysia International Conference*, pp 41-45.
- [10].Singh, S. Gosh, K. Prathyush, SuyashRajan, SagarSuthram, A. Chakrabarty, S. Sanyal, Design of a microstrip patch antenna array using IE3D Software.
- [11].Tiang, J. J., M. T. Islam, N. Misran, and J.S. Mandeep, "Circular Microstrip slot antenna for dual-frequency RFID application". *Progress In Electromagnetics Research*, Vol, 120, 499-512, 2011.
- [12].Wu, C.-M., "Dual-band CPW –fed cross-slot monopole antenna for WLAN operation", *Microwaves, Antennas & Propagation, IET*, Vol. 1, NO. 2, 541-546, April 2007.